JACS
JOURNAL OF THE AMERICAN CHEMICAL SOCIETY

ARTICLE

pubs.acs.org/JACS

A Multiunit Catalyst with Synergistic Stability and Reactivity: A Polyoxometalate–Metal Organic Framework for Aerobic Decontamination

Jie Song,[†,§] Zhen Luo,[†,§] David K. Britt,[‡] Hiroyasu Furukawa,[‡] Omar M. Yaghi,[‡] Kenneth I. Hardcastle,[†] and Craig L. Hill*[,†]

[†]Department of Chemistry, Emory University, Atlanta, Georgia 30322, United States

[‡]Department of Chemistry and Biochemistry, University of California, Los Angeles, Los Angeles, California 90095, United States

Supporting Information

ABSTRACT: A combination of polyanion size and charge allows the Keggin-type polyoxometalate (POM), $[CuPW_{11}O_{39}]^{5-}$, a catalyst for some air-based organic oxidations, to fit snuggly in the pores of MOF-199 (HKUST-1), a metal–organic framework (MOF) with the POM counter-cations residing in alternative pores. This close matching of POM diameter and MOF pore size in this POM–MOF material, $[Cu_3(C_9H_3O_6)_2]_4[\{(CH_3)_4N\}_4CuPW_{11}O_{39}H]$ (**1**), results in a substantial synergistic stabilization of both the MOF and the POM. In addition, this heretofore undocumented POM–MOF interaction results in a dramatic increase in the catalytic turnover rate of the POM for air-based oxidations. While **1** catalyzes the rapid chemo- and shape-selective oxidation of thiols to disulfides and, more significantly, the rapid and sustained removal of toxic H_2S via $H_2S + 1/2\ O_2 \rightarrow 1/8\ S_8 + H_2O$ (4000 turnovers in <20 h), the POM or the MOF alone is catalytically slow or inactive. Three arguments are consistent with the catalytic reactions taking place inside the pores. POM activation by encapsulation in the MOF likely involves electrostatic interactions between the two components resulting in a higher reduction potential of the POM.

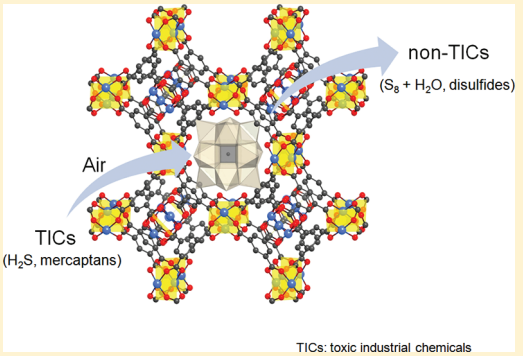

INTRODUCTION

Metal–organic frameworks (MOFs) as a class of crystalline materials offer high levels of porosity with considerable control over pore size and composition.[1−14] Such properties have led to the successful application of MOFs in gas adsorption,[15−20] separation,[21−23] magnetism studies,[24,25] nonlinear optical properties,[26] and more recently catalysis. Several noteworthy studies on MOF-based catalysis are now published.[11−13,27−30] POMs have been successfully incorporated by covalent, electrostatic, and other means into coordination polymers and large pore MOFs,[10,31−40] and some POM-containing structures catalyze oxidation reactions.[31,33−35,38] Recent publications report sorption and hydrolysis of nerve agents by MOFs.[18−20,41,42]

However, there remain two challenges in MOF catalysis that are both addressed in this study: making MOF derivatives that can catalyze reactions using the ambient environment and making MOF catalysts more stable. Catalytic oxidations based on ambient air are of considerable interest because they promise the removal of many toxic or odorous molecules using only air without the need for energy sources, solvents, or other reactives. Oxidizable undesirable compounds include toxic industrial chemicals, chemical warfare agents, indoor air contaminants, and many environmental pollutants.[43,44]

A logical approach to such effective aerobic oxidation catalysts would be to combine the high catalytic activity of particular POMs[45−51] for aerobic oxidations[43,52−55] with the porosity and selective sorption properties of MOFs[4−7] by encapsulating POM catalysts into appropriate MOFs. We henceforth refer to these materials as "POM–MOFs" and note that optimal POM retention logically requires MOF apertures smaller than the POM (with counterions) radius, although one type of POM–MOF has shown negligible loss of POM despite a MOF aperture size larger than the POM radius.[35,38,56] We report here that a MOF with pore sizes closely matching a POM guest self-assembles around this guest to make a material, unlike the POM–MOFs reported in the literature thus far, that has significantly different properties than either the POM or MOF component alone. Specifically, MOF-199 (also known as HKUST-1)[57] in the presence of $[CuPW_{11}O_{39}]^{5-}$ forms a POM–MOF material, $[Cu_3(C_9H_3O_6)_2]_4[\{(CH_3)_4N\}_4CuPW_{11}O_{39}H]\cdot 40H_2O$ (**1**), whose hydrolytic stability is far greater than that of either the MOF or the POM alone and whose strong POM–MOF interactions also dramatically (two orders of magnitude) increase

Received: April 21, 2011
Published: September 13, 2011

the rate of air-based oxidations catalyzed by the POM guest, $[CuPW_{11}O_{39}]^{5-}$ (shape-selective thiol oxidation and fast, sustained decontamination of the toxic industrial chemical H_2S, forming S_8 and water).

EXPERIMENTAL SECTION

General Methods and Materials. MOF-199, PW_{12}-MOF ($[PW_{12}O_{40}]^{3-}$, the saturated parent Keggin-type polyanion of $[CuPW_{11}O_{39}]^{5-}$, in MOF-199), $K_5[CuPW_{11}O_{39}]$, and $TBA_5[CuPW_{11}O_{39}]$ were prepared according to the literature methods,[36,57,58] and their purity was confirmed by Fourier transform infrared (FT-IR) and powder X-ray diffraction (XRD). The other reagents, including $H_3PW_{12}O_{40}$, trimesic acid, $(CH_3)_4NOH$, $Cu(NO_3)_2$, and the thiols were purchased from Aldrich and used without further purification. Gas chromatography (GC) was performed on a Hewlett-Packard 5890 gas chromatograph equipped with a 5% phenyl methyl silicone capillary column, flame ionization detector, and a Hewlett-Packard 3390A series integrator using N_2 as the carrier gas. Elemental analyses for C, H, and N were performed by Atlantic Microlab (Norcross, GA), and K, Na, Cu, P, and W were performed by Galbraith Laboratories (Knoxville, TN). The inductively coupled plasma (ICP) analysis of Cu in the filtrate after catalysis was performed by Columbia Analytical Services (Kelso, WA). The infrared spectra (2% sample in KBr pellet) were recorded on a Nicolet 6700 FT-IR spectrometer from ThermoElectron Corporation. The thermogravimetric data were collected on an ISI TGA 1000 instrument. Powder XRD was measured on a D8 Discover Powder Instrument on monochromatic Cu Kα (λ = 1.54060 Å) radiation. Nitrogen isotherms were collected on Quantachrome AUTOSORB-1 automatic volumetric adsorption instrument.

Synthesis of $[Cu_3(C_9H_3O_6)_2]_4[\{(CH_3)_4N\}_4CuPW_{11}O_{39}H]\cdot 40H_2O$ (1). To 10 mL of distilled water was added $Cu(NO_3)_2\cdot 2.5H_2O$ (480 mg, 2.50 mmol) and $K_5CuPW_{11}O_{39}$ (400 mg, 0.14 mmol), and the resulting blue solution was stirred for 10 min. Trimesic acid (420 mg, 2.0 mmol) and then $(CH_3)_4NOH$ (362 mg, 2.0 mmol) were added sequentially, with 10 min of stirring after each addition. The resulting solution with pH ~ 3 was transferred to a Teflon-lined Parr bomb, heated up to 200 °C for 16 h, programmatically cooled down to 100 °C for another 4 h, and left to cool to ambient temperature. The resulting polyhedron-like deep-blue crystals were separated from the solution and washed with distilled water several times. Further purification was carried out by soaking the crystals in saturated KCl solution and distilled water and sonicating them at least 3 times for 30 min each time to exchange and remove any free metal ions. The product was dried in vacuo overnight to remove water molecules trapped in the pores of the product. Yield: 200 mg (ca. 25% based on POM). Elemental analysis calcd (found %) for $C_{88}H_{153}N_4O_{127}Cu_{13}PW_{11}$ (**1**): calcd for C, 17.11; H, 2.50; N, 0.91; Cu, 13.37; W, 32.73; found for C, 15.85; H, 2.43; N, 0.92; Cu, 12.3; W, 35.1; FT-IR (cm^{-1}): 1649(s), 1452(m), 1374(s), 1080 (w), 987 (w), 898(w), 824(m), 752 (m), 728(m), 497(w).

X-ray Crystallography. An X-ray quality crystal of **1** was coated with Paratone N oil and mounted on a small fiber loop for index and intensity data collection. The XRD data were collected under a nitrogen stream at 173 K on a Bruker D8 SMART APEX CCD single-crystal diffractometer using Mo Kα (0.71073 Å) radiation. Data collection, indexing, and initial cell refinements were processed using the SMART[59] software. Frame integration and final cell refinements were carried out using the SAINT[59] software. The final cell parameters were determined from the least-squares refinement of total reflections. The structures were determined through direct methods (SHELXS97) for locating the tungsten atoms and difference Fourier maps (SHELXL97). The final results of the refinement are listed in Table 1.

Stability Tests of $K_5[CuPW_{11}O_{39}]$ and the POM−MOF, 1. The stability of $K_5[CuPW_{11}O_{39}]$ (10 mg in 1.0 mL of buffer) at different pH values was monitored by UV−vis spectroscopy. The POM−MOF complex, **1** (10 mg), was suspended in 1.0 mL of buffer at pH 7.0 (0.02 M sodium phosphate, NaPi, buffer), pH 8.0 (0.01 M NaPi buffer), pH 9.0 (0.01 M NaPi buffer), pH 10.0 (0.01 M Na borate buffer), and pH 11.0 (0.01 M NaOH). After 12 h, the solids were separated by centrifugation, and the reflection IR spectra were measured using a Nicolet 6700 FT-IR with smart orbital attenuated total reflection (ATR) accessory.

Table 1. Crystallographic Data and Structure Refinement for 1

	1
empirical formula	$C_{88}H_{153}Cu_{13}N_4O_{127}PW_{11}$
formula weight	6178.48 g mol^{-1}
crystal system	cubic
space group	$Fm\bar{3}m$
unit cell	a = 26.307(2) Å
	α = 90°
volume	18 207(3) $Å^3$
Z	4
density (calcd)	2.254 g cm^{-3}
temperature	173(2) K
wavelength	0.71073 Å
abs. coeff	8.500 mm^{-1}
reflections collected	78 158
independent reflections	1448 [R(int) = 0.1396]
GOF	1.040
final R_1[a] [$I > 2\sigma(I)$]	0.0567
final wR_2[b] [$I > 2\sigma(I)$]	0.1788

[a] $R_1 = \Sigma||F_0| - |F_c||/\Sigma|F_0|$. [b] $wR_2 = \Sigma[w(F_0^2 - F_c^2)^2]/\Sigma[w(F_0^2)^2]^{1/2}$.

Catalytic Experiments. *Aerobic H_2S Oxidation in Aqueous Solution.* In a typical reaction, the catalyst (10.0 mg) was weighed and added to a clean, dry pressure tube, and the complete experimental assembly was flushed with oxygen or air and weighed. The reaction was initiated by addition of a saturated aqueous solution of H_2S (0.1 mol/L, pH = 4.8, 75 mL). The reaction vessel was then sealed quickly, and the reaction solution was stirred at room temperature for 20 h. After several minutes, the clear colorless solution became cloudy, and the yellow elemental sulfur began to precipitate on the walls of reaction vial. The solid reaction mixture, in parallel reactors for each specific reaction period, was separated by centrifugation, dried in vacuum overnight, and weighed.

Aerobic H_2S Oxidation under Gas Phase (Solvent-Free). In a typical reaction, the catalyst (150.0 mg) was weighed in a beaker and then placed in a desiccator. The H_2S gas was generated by mixing of solid K_2S (0.5051 g) with H_3PO_4 (100 mL) in another beaker and placed in the same desiccator, and then the cap of the desiccator was sealed tightly. The H_2S gas was circulated by a fan in the desiccator. Reaction with the dioxygen in the air takes place on the surface of the catalyst particles. After one week, the catalyst was dried and characterized by FT-IR. The weight of catalyst before and after reaction was assessed carefully three times.

Aerobic Thiol Oxidation. In a typical catalytic thiol oxidation experiment, 60.0 μL (6.62×10^{-4} mol) of propanethiol (PrSH), 18.0 μL (9.2×10^{-5} mol) of decane (internal standard), and 10 mg of **1** were stirred in 2.9 mL of chlorobenzene in a Schlenk tube fitted with poly(tetrafluoroethylene) (PTFE) septum stopper under dioxygen at 45 °C for 5 days. Aliquots were withdrawn from the Schlenk tube at approximately 10 h intervals, and the products were quantified by gas chromatography. Before the withdrawal of each aliquot, the reaction solution was placed in an ice−water bath for 20 min to minimize loss of the volatile PrSH. After opening the Schlenk tube, 0.1 μL of cooled reaction solution was withdrawn as quickly as possible, and the atmosphere in the tube was carefully filled with dioxygen gas.

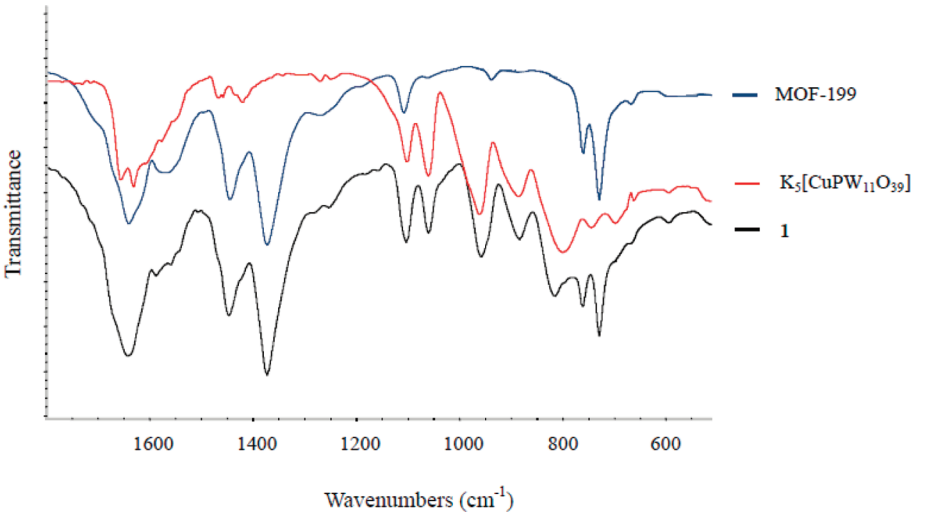

Figure 1. FT-IR spectra of MOF-199 alone (blue), $K_5[CuPW_{11}O_{39}]$ alone (red), and **1** (black).

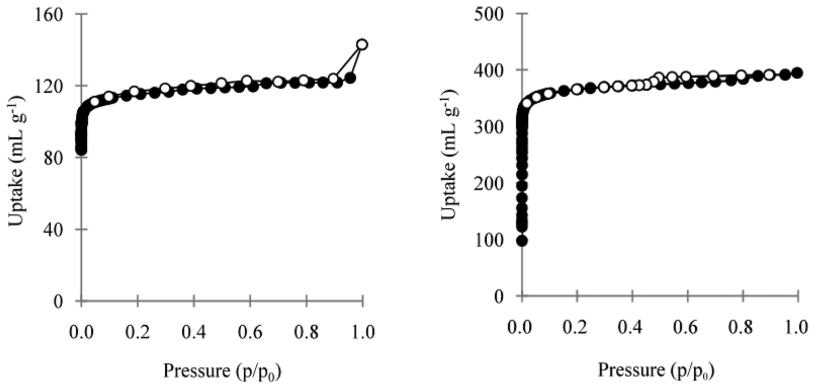

Figure 2. N_2 gas adsorption isotherms of **1** (left) and MOF-199 (right) measured at 77 K. Filled symbols, adsorption; open symbols, desorption. The BET surface areas of **1** and MOF-199 alone are 462 and 1264 m^2/g, respectively.

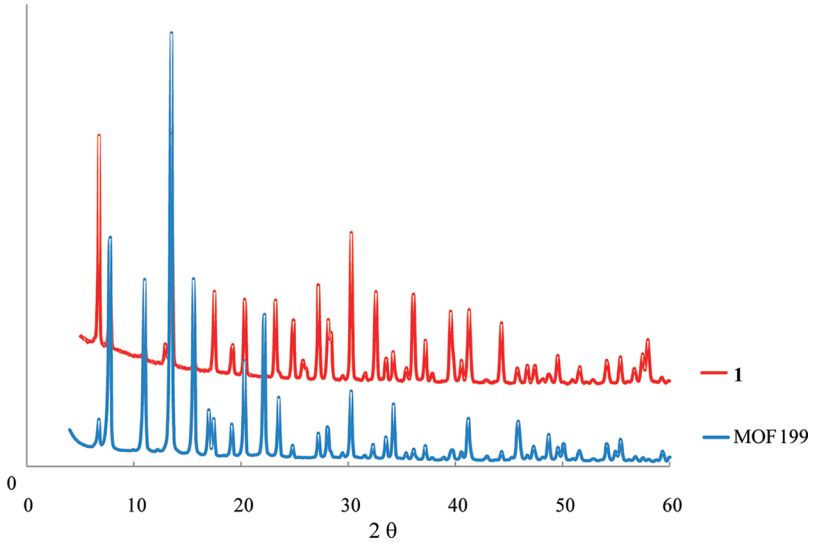

Figure 3. Powder XRD patterns of **1** and MOF-199.

dx.doi.org/10.1021/ja203695h |*J. Am. Chem. Soc.* 2011, 133, 16839–16846

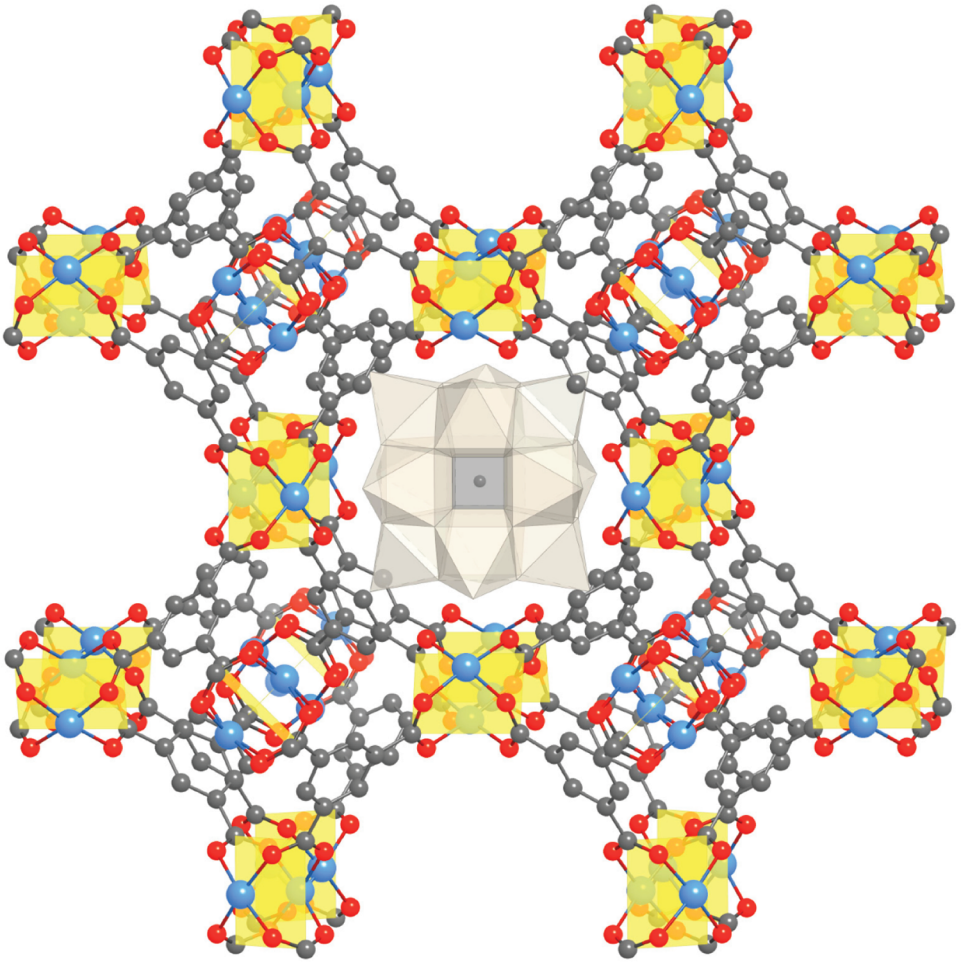

Figure 4. X-ray crystal structure of **1**. The POM, represented as off-white polyhedra, is orientationally disordered in the pores. The MOF-199 framework is represented in ball and stick form, wherein C atoms are represented in gray, O in red, and Cu in blue. Yellow squares denote the geometry of the copper(II) acetate clusters. TMA cations, which are disordered in the pores, and hydrogen atoms are omitted for clarity.

RESULTS AND DISCUSSION

A solution of $Cu(NO_3)_2 \cdot 2.5H_2O$, $K_5CuPW_{11}O_{39}$, trimesic acid, and $(CH_3)_4NOH$, treated under hydrothermal conditions, results in X-ray quality crystals of the POM−MOF, **1**, in ca. 25% yield (based on POM). These crystals were filtered, washed with distilled water, and dried in vacuum. The FT-IR spectrum of **1** clearly shows the characteristic peaks of both POM and MOF components (Figure 1).[57] Both the UV−vis and FT-IR spectra of the concentrated filtrates from washing the purified **1** with water indicate that no POM whatsoever is lost from **1** by these procedures. The specific surface area of **1**, measured by the Brunauer−Emmett−Teller (BET) method, is 462 m^2/g (Figure 2). The surface area of the POM−MOF is generally one-third that of the isostructural bulk MOF-199 (1264 m^2/g) before guest molecule incorporation.[44,57] The relatively low surface area indicates that most of the MOF pores are occupied by the POM and its counterions. The stoichiometries of formula of **1**, shown in Table 1, were generated and defined on the basis of crystal structure, elemental analysis, and hermogravimetric analysis.

The powder XRD pattern and single crystal X-ray structure of **1** reveal that the parent MOF-199 framework has been maintained and that the catalytically active tetramethylammonium (TMA) salt of the Cu-containing POM, $[CuPW_{11}O_{39}]^{5-}$ has been introduced into this $[Cu_3(C_6H_3O_6)_2]_4$-based MOF (Figures 3 and 4). The structure of **1** clearly reveals the high occupancy of the POMs and their counterions in the pores. Predictably, given the pore and POM volumes, the TMA counterions do not reside in the same pores as the POM polyanions but in adjacent pores. Analysis of the unit cells reveals, in addition to the occupancy of large and small pores by polyanion (POM) units and countercations, respectively, that 50% of the large pores are empty. The pores are connected in nonlinear channels and facilitate reactant access and product departure. Both the transition-metal-substituted POM and countercations are disordered, leading to the location of the N atoms of only two of total four TMA cations. As in nearly all X-ray structures of α-Keggin POMs with one substituted metal-oxo or metal-aqua unit, the polyanion is orientationally disordered so the substituted metal occurs at all 12 Keggin sites. Each encapsulated POM can be accessed via six adjacent pores, which contain the TMA ions.

POM−MOF **1** is capable of catalyzing the air-based oxidative decontamination of toxic sulfur compounds. Hydrogen sulfide is oxidatively converted by **1** under ambient conditions via eq 1 (Figure 5 and Tables 2 and 3) in aqueous solution or gas phase. The resulting yellow powder was confirmed to be elemental sulfur by its UV−vis spectrum after extraction into chloroform

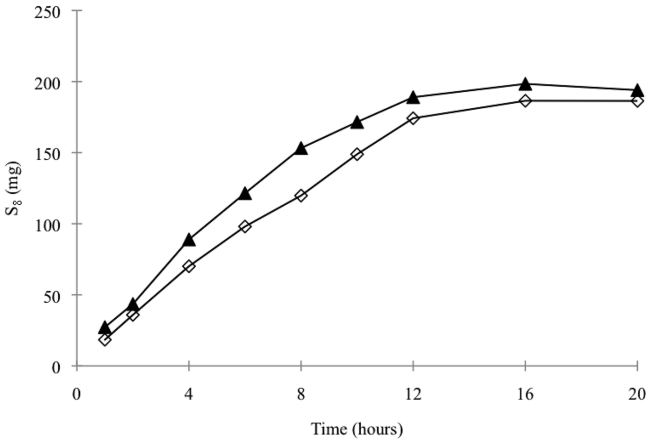

Figure 5. Aerobic oxidation of H_2S to S_8 catalyzed by the POM−MOF, **1**, in water. An aqueous solution of H_2S (0.1 mol/L, pH = 4.8, 75 mL) containing **1** (10.0 mg) was flushed with oxygen (black triangles) or air (open squares) and stirred at room temperature for the duration of the reaction (20 h). Parallel reactions were conducted and stopped at specific reaction times for product separation and measurement. Control experiments for POM (10.0 mg) and MOF-199 (10.0 mg) only under identical conditions showed no catalytic activity (no production of S_8).

Table 2. Quantity of sulfur, Produced via eq 1 in Aqueous Solution, Catalyzed by 10 mg of 1 after 20 h

	weight of S_8(mg)	TON[a]
oxygen-based catalysis	220 ± 30	4300
air-based catalysis	190 ± 20	3800

[a] Turnover number (TON) = moles of H_2S consumed (or 8 × moles of product S_8 formed) per mol of catalyst used.

Table 3. Quantity of Sulfur, Produced via eq 1 in Gas Phase under Ambient Conditions, Catalyzed by 1, PW_{12}-MOF, MOF-199, and $\{CuPW_{11}\}$

	catalysts (mg)	S_8 formed (mg)	TON[a]
1	150	9.5 ± 0.1	12.0
PW_{12}-MOF	150	0.2 ± 0.1	0.2
MOF-199	150	0.2 ± 0.1	0.02
$\{CuPW_{11}\}$	150	–[b]	–

[a] Turnover number (TON) = moles of H_2S consumed (or 8 × moles of product S_8 formed) per mol of catalyst used. [b] No detectable weight change when $\{CuPW_{11}\}$ was used as catalyst

solution. The turnover number (TON), based on H_2S consumed (1/8 S_8 formed) and POM units present in **1**, is ca. 4000 in less than 20 h in aqueous solution. In aqueous solution, the product inhibition (blockage of the pores in **1** by marginally soluble S_8 product) does little to inhibit the reaction at the outset, and FT-IR shows that the integrity of the POM−MOF structure is maintained during reaction (see Figure S1 in Supporting Information):

$$H_2S + 1/2\,O_2(\text{air}) \rightarrow 1/8\,S_8 + H_2O \quad (1)$$

Control experiments in aqueous solution using $K_5[CuPW_{11}O_{39}]$ only or, separately, MOF-199 only showed no production of solid S_8. Additional experiments showed that the solid MOF decomposes in minutes based on both color change (blue to colorless) and dissolution of the material in the reaction solution (H_2O, pH 4.8). The POM−MOF was reproducibly much more stable to decomposition than the same MOF alone (no POM guest). The H_2S oxidation in gas phase catalyzed by **1** also exhibits the synergetic effects. No or very few oxidation products were detected in control experiments. Interestingly, the non-copper-containing polyanion, PW_{12}-MOF, showed very low activity in catalyzing H_2S oxidation. These results indicate that the Cu centers in the POM unit of **1** are very likely the active site for the H_2S oxidation. Production of S_8 by **1** in the gas phase stopped at TON ~ 12, in contrast to the aqueous solution H_2S oxidations, as expected because of the blockage of the pores in **1** by the oxidation product.

To assess the ability of **1** to catalyze other aerobic oxidations, the conversion of volatile mercaptans to less toxic and odorous disulfides was examined. Removal of sulfur-based harmful industrial chemicals[60,61] is important in the deodorization and jet fuel sweetening industries.[62−64] Aerobic mercaptan oxidation catalyzed by **1** was established to proceed readily under ambient conditions via the stoichiometry in eq 2:

$$2\,RSH + 1/2\,O_2 \rightarrow RSSR + H_2O \quad (2)$$

Figure 6 shows the air-based oxidation of propanethiol (PrSH) in chlorobenzene solution catalyzed by **1**. Di-*n*-propyl disulfide was the only product detected by gas chromatography and mass spectrometry. Under the same reaction conditions where **1** produces 200 turnovers, the production of disulfide is negligible in the absence of the catalyst. Significantly, the activity of an equimolar amount of the tetrabutylammonium salt of the monocopper-substituted-POM, $TBA_5[CuPW_{11}O_{39}]$, (homogeneous catalyst), POM-free MOF-199, and PW_{12}-MOF (heterogeneous) under identical conditions was assessed and shown to be ca. one order of magnitude lower than that of the new material, **1**, itself. Immobilization of homogeneous catalysts usually results in turnover rates that are one to three orders of magnitude lower than those for the same catalyst in solution, although we have noted modest increases in turnover rates when some POM catalysts are immobilized on cationic surfaces.[52,65,66] It is likely that electrostatic interactions between the solvent-accessible Cu(II) centers of the MOF structure and the encapsulated $[CuPW_{11}O_{39}]^{5-}$ units are present in **1**, and these stabilize **1** relative to its components. Such electrostatic POM−MOF interactions could simultaneously increase the potential of the Cu centers in the POM unit of **1**, which would be expected to increase the rates of the substrate oxidation-$[CuPW_{11}O_{39}]^{5-}$ reduction step in the overall oxidations catalyzed by the POM−MOF. Reoxidation of Cu(I) centers in the reduced POM units of **1** by O_2 is not rate limiting because the overall oxidation rates are independent of O_2 pressure. The chemistry of thiol oxidation is well-known to proceed through one-electron oxidized sulfur-based intermediates, and sulfide oxidation is very similar. The mechanism for S_8 formation clearly involves multiple steps and will be addressed in subsequent work.

Table 4 summarizes the air-based oxidations of representative mercaptans varying in electron density, nucleophilicity, and steric bulk around the sulfur atom catalyzed by **1** under similar conditions. Gas chromatographic analyses confirm the 99% chemo-selective oxidation of all the evaluated mercaptans to disulfides. In addition, size- and shape-dependent selectivity is

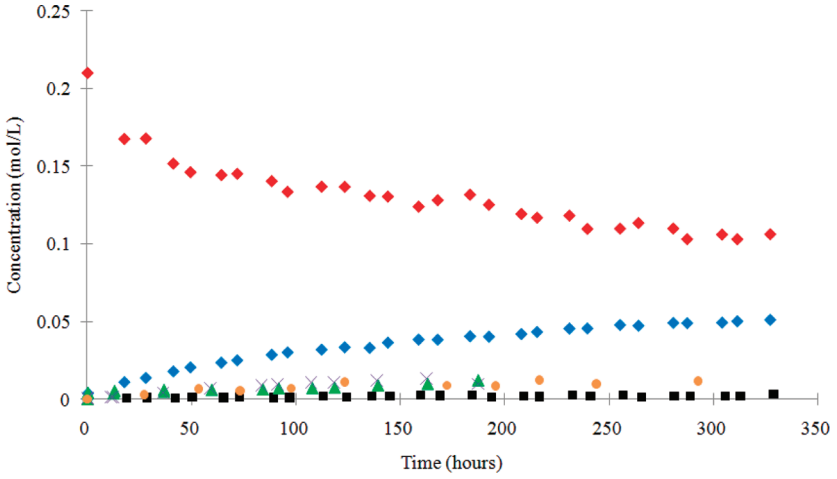

Figure 6. Aerobic oxidation of PrSH to PrSSPr catalyzed by **1**. PrSH (0.662 mmol) and the catalyst, **1** (10 mg, ~0.0016 mmol), were stirred in chlorobenzene (2.9 mL) with decane (internal standard, 0.092 mmol) in a pressure tube (45 mL) fitted with a PTFE plug under 100% O_2 at 50 °C. Consumption of PrSH (red diamonds) and formation of PrSSPr (blue diamonds) catalyzed by **1**; PrSSPr concentration in presence of PW_{12}-MOF (orange circle); PrSSPr concentration in presence of MOF-199 alone (green triangle); PrSSPr concentration in presence of $TBA_5[CuPW_{11}O_{39}]$ alone (purple crosses); and PrSSPr concentration in absence of any additives (black squares).

Table 4. Aerobic Oxidation of Thiols to Disulfides Catalyzed by 1[a]

Substrates	Products	Selectivity	Conversions
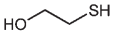	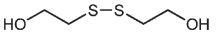	99%	95%
	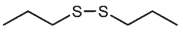	99%	77%
	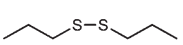	99%	37%
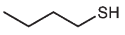	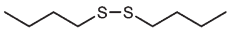	99%	32%
	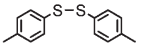	99%	27%

[a] Conversion measured after 62 h. In a typical kinetic experiment, substrate thiol (6.5×10^{-4} mol), decane (18.0 μL, 9.2×10^{-5} mol, internal standard), and **1** (10 mg) were stirred in chlorobenzene (2.9 mL) in a pressure tube (45 mL) fitted with a PTFE septum stopper under O_2 or air (both give very similar results) at 45 °C. A control reaction conducted under the same conditions except without catalyst showed no oxidation products whatsoever.

clearly observed in these reactions. 2-Hydroxyethanethiol gives the highest conversion (95%), while *p*-toluenethiol gives less than a 30% yield of disulfide. Conversions decrease with an increase in the number of mercaptan carbon atoms. This is consistent with thiol oxidation by the POM units encapsulated in the MOF: sterically larger thiols are less accessible to the POM units and thus are oxidized at lower rates. The disulfide products are also obtained in proportionally lower yields. The higher conversion for oxidation of 2-hydroxyethanethiol relative to other thiols is attributed to the higher affinity of this hydrogen-bonding thiol for the hydrophilic channels in the MOF. Again, the rates of propanethiol oxidation under air and pure O_2 catalyzed by **1** are very similar, indicating that POM reduction, and not reduced POM reoxidation by O_2, is rate limiting.

The used catalyst, **1**, is readily separated from the catalytic oxidations described above by filtration. The separated supernatant of the reaction solution shows no catalytic activity for any of the aerobic oxidations reported here. The isolated catalyst was reused for these reactions after simple filtration, washing with dichloromethane, and drying. The electronic absorption spectrum and the ICP analysis of Cu (Table S1, Supporting Information) of the dichloromethane filtrate shows no leaching of the POM from **1** whatsoever.

Significantly, the integrated ensemble, **1**, is very robust in both aqueous and organic solutions during the catalysis. Enhanced structural and hydrolytic stability of both $[CuPW_{11}O_{39}]^{5-}$ and MOF-199 in **1** relative to the POM alone (i.e., the K_5 salt) or the MOF alone is clearly observed over a wide pH range. $[CuPW_{11}O_{39}]^{5-}$ is hydrolytically stable in solution only from pH 2.0 to 5.9[58] and decomposes quickly in basic aqueous solution. MOF networks usually exist in a much narrower pH range, and the host framework used, MOF-199, has been determined to be only metastable at pH 4.0. In contrast, both the FT-IR and UV−vis spectra demonstrate that $[CuPW_{11}O_{39}]^{5-}$ when present in **1** remains intact at pH 11.0 for at least 12 h (see Figure S2, Supporting Information). This dramatic enhancement of POM stability upon incorporation into some MOFs has positive implications for catalytic and other applications.[67,68]

Three lines of additional evidence indicate that **1** stays intact during the catalytic oxidation: (1) The recycled **1** catalyzes aerobic oxidation of H_2S and propanethiol for at least three cycles without significant activity loss; (2) the FT-IR of **1** after reaction retains all the characteristic peaks of the polyanion, $[CuPW_{11}O_{39}]^{5-}$, and MOF-199, indicating that both structural components are stable (see Figure S3, Supporting Information); and (3) the X-ray powder diffraction patterns of **1** before and after use as a catalyst are identical (see Figure S4, Supporting Information).

The present study clearly documents a new type of robust catalyst that exhibits the attractive features of both its components, the POM and the MOF, shows mutual enhancement of stability by each component, and efficiently catalyzes the detoxification of various sulfur compounds including H_2S to S_8 using only ambient air. Significantly, the synergy between the two structural components of **1** also extends to the catalytic activity of the polyanion: The $\{CuPW_{11}\}$ in **1** is one to several orders of magnitude faster under otherwise identical conditions in these

aerobic oxidation reactions than in solution. The fact that **1** is a readily reisolated and reused heterogeneous catalyst that requires only the ambient environment for some oxidation processes indicates its potential value as a versatile and robust catalytic decontaminant. Considering that both POMs and MOFs are two large classes of species with different compositions and structures, selective combinations of these two components would be expected to afford many new materials, and this large experimental space could be tuned to target the catalytic removal of a range of other TICs and pollutants using just the ambient environment.

■ ASSOCIATED CONTENT

Supporting Information. Several spectroscopic and thermogravimetric analyses of POM−MOF (**1**) stability in different reactions and conditions, additional control reactions, and ICP analysis of the supernatant after catalysis. This material is available free of charge via the Internet at http://pubs.acs.org.

■ AUTHOR INFORMATION

Corresponding Author
chill@emory.edu

Author Contributions
[§]These authors contributed equally.

■ ACKNOWLEDGMENT

This work was supported by the following grants to C.L.H: HDTRA1-09-1-0002 (from DTRA) and W911NF-05-1-0200 (from ARO) and to O.M.Y: 911NF-06-1-0405 (from ARO). We thank Chongchao Zhao and Sheri Lense for X-ray crystallographic efforts.

■ REFERENCES

(1) Kitagawa, S.; Kitaura, R.; Noro, S.-i. *Angew. Chem., Int. Ed.* **2004**, *43*, 2334.
(2) Long, J. R.; Yaghi, O. M. *Chem. Soc. Rev.* **2009**, *38*, 1213.
(3) Tranchemontagne, D. J.; Mendoza-Cortes, J. L.; O'Keeffe, M.; Yaghi, O. M. *Chem. Soc. Rev.* **2009**, *38*, 1257.
(4) O'Keeffe, M.; Peskov, M. A.; Ramsden, S. J.; Yaghi, O. M. *Acc. Chem. Res.* **2008**, *41*, 1782.
(5) Ockwig, N. W.; Delgado-Friedrichs, O.; O'Keeffe, M.; Yaghi, O. M. *Acc. Chem. Res.* **2005**, *38*, 176.
(6) Eddaoudi, M.; Moler, D. B.; Li, H.; Chen, B.; Reineke, T. M.; O'Keeffe, M.; Yaghi, O. M. *Acc. Chem. Res.* **2001**, *34*, 319.
(7) Yaghi, O. M.; Li, H.; Davis, C.; Richardson, D.; Groy, T. L. *Acc. Chem. Res.* **1998**, *31*, 474.
(8) Czaja, A. U.; Trukhan, N.; Muller, U. *Chem. Soc. Rev.* **2009**, *38*, 1284.
(9) Duan, C.; Wei, M.; Guo, D.; He, C.; Meng, Q. *J. Am. Chem. Soc.* **2010**, *132*, 3321.
(10) Zheng, S. T.; Zhang, J.; Yang, G. Y. *Angew. Chem., Int. Ed.* **2008**, *47*, 3909.
(11) Alaerts, L.; Wahlen, J.; Jacobs, P. A.; Vos, D. E. D. *Chem. Commun.* **2008**, 1727.
(12) Corma, A.; García, H.; Llabrés i Xamena, F. X. *Chem. Rev.* **2010**, *110*, 4606.
(13) Ma, L.; Abney, C.; Lin, W. *Chem. Soc. Rev.* **2009**, *38*, 1248.
(14) Férey, G. *Chem. Soc. Rev.* **2008**, *37*, 191.
(15) Eddaoudi, M.; Kim, J.; Rosi, N.; Vodak, D.; Wachter, J.; O'Keeffe, M.; Yaghi, O. M. *Science* **2002**, *295*, 469.
(16) Murray, L. J.; Dinca, M.; Long, J. R. *Chem. Soc. Rev.* **2009**, *38*, 1294.
(17) Yoon, J. W.; Jhung, S. H.; Hwang, Y. K.; Humphrey, S. M.; Wood, P. T.; Chang, J.-S. *Adv. Mater.* **2007**, *19*, 1830.
(18) Montoro, C.; Linares, F.; Procopio, E. Q.; Senkovska, I.; Kaskel, S.; Galli, S.; Masciocchi, N.; Barea, E.; Navarro, J. A. R. *J. Am. Chem. Soc.* **2011**, *133*, 11888.
(19) Zou, R.; Zhong, R.; Han, S.; Xu, H.; Burrell, A. K.; Henson, N.; Cape, J. L.; Hickmott, D. D.; Timofeeva, T. V.; Larson, T. E.; Zhao, Y. *J. Am. Chem. Soc.* **2010**, *132*, 17996.
(20) Lee, J.-H.; Houk, R. T. J.; Robinson, A.; Greathouse, J. A.; Thornberg, S. M.; Allendorf, M. D.; Hesketh, P. J. In *Micro- and Nanotechnology Sensors, Systems, and Applications II (Proceedings of SPIE)*; George, T., Islam, M. S., Dutta, A. K.; SPIE: Bellingham, WA, 2010; Vol. 7679, p 767927/1; doi:10.1117/12.850217.
(21) Matsuda, R.; Kitaura, R.; Kitagawa, S.; Kubota, Y.; Belosludov, R. V.; Kobayashi, T. C.; Sakamoto, H.; Chiba, T.; Takata, M.; Kawazoe, Y.; Mita, Y. *Nature* **2005**, *436*, 238.
(22) Li, J.-R.; Kuppler, R. J.; Zhou, H.-C. *Chem. Soc. Rev.* **2009**, *38*, 1477.
(23) Chen, B.; Liang, C.; Yang, J.; Contreras, D. S.; Clancy, Y. L.; Lobkovsky, E. B.; Yaghi, O. M.; Dai, S. *Angew. Chem., Int. Ed.* **2006**, *45*, 1390.
(24) Halder, G. J.; Kepert, C. J.; Moubaraki, B.; Murray, K. S.; Cashion, J. D. *Science* **2002**, *298*, 1762.
(25) Cheng, X. N.; Zhang, W. X.; Lin, Y. Y.; Zheng, Y. Z.; Chen, X. M. *Adv. Mater.* **2007**, *19*, 1494.
(26) Evans, O. R.; Lin, W. *Acc. Chem. Res.* **2002**, *35*, 511.
(27) Seo, J. S.; Whang, D.; Lee, H.; Jun, S. I.; Oh, J.; Jeon, Y. J.; Kim, K. *Nature* **2000**, *404*, 982.
(28) Lee, J. Y.; Farha, O. K.; Roberts, J.; Scheidt, K. A.; Nguyen, S. B. T.; Hupp, J. T. *Chem. Soc. Rev.* **2009**, *38*, 1450.
(29) Uemura, T.; Yanai, N.; Kitagawa, S. *Chem. Soc. Rev.* **2009**, *38*, 1228.
(30) Wang, S.; Li, L.; Zhang, J.; Yuan, X.; Su, C.-Y. *J. Mater. Chem.* **2011**, *21*, 7098.
(31) Zeng, H.; Newkome, G. R.; Hill, C. L. *Angew. Chem., Int. Ed.* **2000**, *39*, 1771.
(32) Yang, L.; Naruke, H.; Yamase, T. *Inorg. Chem. Commun.* **2003**, *6*, 1020.
(33) Han, J. W.; Hardcastle, K. I.; Hill, C. L. *Eur. J. Inorg. Chem.* **2006**, 2598.
(34) Han, J. W.; Hill, C. L. *J. Am. Chem. Soc.* **2007**, *129*, 15094.
(35) Maksimchuk, N. V.; Timofeeva, M. N.; Melgunov, M. S.; Shmakov, A. N.; Chesalov, Y. A.; Dybtsev, D. N.; Fedin, V. P.; Kholdeeva, O. A. *J. Catal.* **2008**, *257*, 315.
(36) Sun, C.-Y.; Liu, S.-X.; Liang, D.-D.; Shao, K.-Z.; Ren, Y.-H.; Su, Z.-M. *J. Am. Chem. Soc.* **2009**, *131*, 1883.
(37) Yu, R.; Kuang, X.-F.; Wu, X.-Y.; Donahue, J. P. *Coord. Chem. Rev.* **2009**, *253*, 2872.
(38) Maksimchuk, N. V.; Kovalenko, K. A.; Arzumanov, S. S.; Chesalov, Y. A.; Melgunov, M. S.; Stepanov, A. G.; Fedin, V. P.; Kholdeeva, O. A. *Inorg. Chem.* **2010**, *49*, 2920.
(39) Inman, C.; Knaust, J. M.; Keller, S. W. A. *Chem. Commun.* **2002**, 156.
(40) Murakami, M.; Hong, D.; Suenobu, T.; Yamaguchi, S.; Ogura, T.; Fukuzumi, S. *J. Am. Chem. Soc.* **2011**, *133*, 11605.
(41) Ni, Z.; Jerrell, J. P.; Cadwallader, K. R.; Masel, R. I. *Anal. Chem.* **2007**, *79*, 1290.
(42) Ma, F.-J.; Liu, S.-X.; Sun, C.-Y.; Liang, D.-D.; Ren, G.-J.; Wei, F.; Chen, Y.-G.; Su, Z.-M. *J. Am. Chem. Soc.* **2011**, *133*, 4178.
(43) Hill, C. L.; Okun, N. M.; Hillesheim, D. A.; Geletii, Y. V. In *Anti-Terrorism and Homeland Defense: Polymers and Materials, ACS Symposium Series 980, Chapter 12*; Reynolds, J. G., Lawson, G. E., Koester, C. J., Eds.; American Chemical Society: Washington, D.C., 2007, p 198.
(44) Britt, D.; Tranchemontagne, D.; Yaghi, O. M. *Proc. Natl. Acad. Sci. U.S.A.* **2008**, *105*, 11623.
(45) Nohra, B.; El Moll, H.; Rodriguez-Albelo, L. M.; Mialane, P.; Marrot, J.; Mellot-Draznieks, C.; O'Keeffe, M.; Biboum, R. N.; Lemaire, J.; Keita, B.; Nadjo, L.; Dolbecq, A. *J. Am. Chem. Soc.* **2011**, *133*, 13363.

(46) Pope, M. T.; Müller, A. *Angew. Chem., Int. Ed. Engl.* **1991**, *30*, 34.
(47) Borrás-Almenar, J. J.; Coronado, E.; Müller, A.; Pope, M. T. *Polyoxometalate Molecular Science*; Kluwer Academic Publishers: Dordrecht, The Netherlands, 2003; Vol. 98.
(48) Hill, C. L. In *Comprehensive Coordination Chemistry-II: From Biology to Nanotechnology*; Wedd, A. G., Ed.; Elsevier Ltd.: Oxford, U.K., 2004; Vol. 4, p 679.
(49) Pope, M. T. In *Comprehensive Coordination Chemistry II: From Biology to Nanotechnology*; Wedd, A. G., Ed.; Elsevier Ltd.: Oxford, U.K., 2004; Vol. 4, p 635.
(50) Kögerler, P.; Cronin, L. *Angew. Chem., Int. Ed.* **2005**, *44*, 844.
(51) Long, D.-L.; Burkholder, E.; Cronin, L. *Chem. Soc. Rev.* **2007**, *36*, 105.
(52) Okun, N. M.; Anderson, T. M.; Hill, C. L. *J. Mol. Catal. A: Chem.* **2003**, *197*, 283.
(53) Kholdeeva, O. A.; Timofeeva, M. N.; Maksimov, G. M.; Maksimovskaya, R. I.; Neiwert, W. A.; Hill, C. L. *Inorg. Chem.* **2005**, *44*, 666.
(54) Okun, N. M.; Tarr, J. C.; Hilleshiem, D. A.; Zhang, L.; Hardcastle, K. I.; Hill, C. L. *J. Mol. Catal. A: Chem.* **2006**, *246*, 11.
(55) Hill, C. L. *J. Mol. Catal. A: Chem.* **2007**, *262*, 2.
(56) Férey, G.; Mellot-Draznieks, C.; Serre, C.; Millange, F.; Dutour, J.; Surblé, S.; Margiolaki, I. *Science* **2005**, *309*, 2040.
(57) Chui, S. S.-Y.; Lo, S. M.-F.; Charmant, J. P. H.; Orpen, A. G.; Williams, I. D. *Science* **1999**, *283*, 1148.
(58) Tourné, C. M.; Tourné, G. F.; Malik, S. A.; Weakley, T. J. R. *J. Inorg. Nucl. Chem.* **1970**, *32*, 3875.
(59) SAINT, ver. 6.28 and SMART, ver. 5.628, *Bruker AXS* Analytical X-ray Sysems: Madison, WI, 2003.
(60) Xu, L.; Boring, E.; Hill, C. *J. Catal.* **2000**, *195*, 394.
(61) Hill, C. L.; Anderson, T. M.; Han, J.; Hillesheim, D. A.; Geletii, Y. V.; Okun, N. M.; Cao, R.; Botar, B.; Musaev, D. G.; Morokuma, K. *J. Mol. Catal. A: Chem.* **2006**, *251*, 234.
(62) In *Profile of the Petroleum Refining Industry*; EPA: Washington, D.C., 1995; p 30.
(63) Basu, B.; Satapathy, S.; Bhatnagar, A. K. *Catal. Rev., Sci. Eng.* **1993**, *35*, 571.
(64) Leitao, A.; Rodrigues, A. *Chem. Eng. Sci.* **1990**, *45*, 679.
(65) Okun, N. M.; Anderson, T. M.; Hill, C. L. *J. Am. Chem. Soc.* **2003**, *125*, 3194.
(66) Okun, N. M.; Ritorto, M. D.; Anderson, T. M.; Apkarian, R. P.; Hill, C. L. *Chem. Mater.* **2004**, *16*, 2551.
(67) Cho, S.-H.; Ma, B.; Nguyen, S. T.; Hupp, J. T.; Albrecht-Schmitt, T. E. *Chem. Commun.* **2006**, 2563.
(68) Isaeva, V. I.; Kustov, L. M. *Pet. Chem.* **2010**, *50*, 167.